WARSAW UNIVERSITY OF TECHNOLOGY Index 351733
FACULTY OF CIVIL ENGINEERING
COMMITTEE FOR CIVIL AND WATER ENGINEERING
POLISH ACADEMY OF SCIENCES ISSN 1230-2945

DOI: 10.24425/ace.2021.138522

ARCHIVES OF CIVIL ENGINEERING

Vol. LXVII ISSUE 4 2021

pp. 625 –642

Research paper

Fatigue safety verification of riveted steel railway bridges using probabilistic method and standard S–N curves

Anna Maria Rakoczy[1]

Abstract: The current fatigue evaluation procedures in Europe and North American bridge codes do not account for the degree of uncertainty in load and resistance models. However, the variability of cycling loading and material properties have a significant influence on fatigue safety verification. A fatigue verification is contingent on the accumulated load cycles and the fatigue category; which, in turn, depends on member type and its connections. Assessment of structural safety can be evaluated more completely using probabilistic methods that provide fatigue prediction in terms of the probability of crack initiation. This method provides more information about the expected performance of a structural component; therefore, the structure can be used in service for a significantly longer time. In this article, the comparison of fatigue evaluation is presented using Eurocode, North American Standard – AREMA, and the new approach using the probabilistic method. These methods are demonstrated on the riveted built-up beams of the steel deck plate girder (DPG) railway bridge using data from field monitoring.

Keywords: railroad bridges, riveted steel structures, measured strains, cyclic loads, fatigue safety, remaining safe service life

[1]PhD., Eng., Research Assistant Professor, Road and Bridge Research Institute, ul. Instytutowa 1., 03-302 Warsaw, Poland, e-mail: arakoczy@ibdim.edu.pl, ORCID: 0000-0003-1208-5729

1. Introduction

The problem with the degradation process of railway bridges is becoming a more important issue in almost all European countries [1] and around the world [2, 3]. In Europe more than 35 percent of railway bridges and viaducts are more than 100 years old [1]; while in North America, more than 50 percent are over 100 years old, and the oldest bridges are close to 150 years old [2]. Deterioration is a part of the aging process of all structures; however, the degradation mechanism is different for each bridge type, length, and structural material. During the service time, the bridge structures are exposed to numerous live loads and environmental cycles that can reduce the bridge capacity. The cycling loading, that yields tensile stress, is also a cause of fatigue crack initiation. Each additional tensile stress cycle is causing incremental growth of the fatigue crack that eventually can provide to fracture and a failure of a component. Therefore, there is a growing need to develop efficient procedures for the evaluation and prediction of a remaining service for these aging structures.

Among these aging structures, short and medium steel spans dominate. They are usually built from two main plate girders which are typically I-beams made up of separate structural steel plates (so-called: built-up sections), that are welded, bolted, or riveted together to form the vertical web and horizontal flanges of the beam [4]. In the railroad deck-type bridge (DPG), the railroad ties themselves may form the bridge deck (Fig. 1), or the deck may support the ballast on which the track is placed.

Fig. 1. A typical riveted DPG spans with an open deck (no ballast)

In the past decade, several riveted steel DPG railway bridge spans were tested and analyzed for fatigue and safe service performance under the research program sponsored by the Association of American Railroads (AAR) [5]. The research findings confirmed that simplified calculations and conservative assumptions lead to significant reductions in the estimated safety of the structure. The current methods for fatigue evaluation indicate a low probability of fatigue, which means that even if the bridge reaches a fatigue limit, the structure is likely to be fit for future service with more frequent inspection [6]. The American Railway Engineering and Maintenance of Way Association (AREMA) *Manual for Railway Engineering*, Chapter 15 calculations recommended practice for fatigue evaluation is based on S–N curves developed by using 95 percent confidence limits for 97.5 percent survival applied to full-scale test data [7]. Also, in European standards [8, 9], the durability of the bridge is most often determined with a confidence level equal to 95%. Therefore, when the durability reaches its limit, the damage may occur in more than 5% of the bridge structural elements, that further depends whether the elements are in series or parallel, e.g., cracks in joints, rivets, or prestressing bolts and cracks in the concrete slab [10]. However, if the fatigue assessment revealed with high probability that initiation and propagation of fatigue cracks were likely to take place in some non-redundant members within the actual structural system, it constitutes a high risk of a collapse of the bridge and compromises the safety of users [11].

Many factors influence fatigue verification of riveted historical metal bridges and are considered by many researchers (see among others: [12–15]). One of them is the uncertainty in the fatigue model that has a significant influence on the fatigue evaluation [16]. The reliability approach for railway bridges was first introduced in Europe by Brühwiler and Kunz [17]. Then, a reliability-based method for fatigue evaluation of railway bridges was presented in the U.S. [18]. The deterministic fatigue assessment of simply supported, short-span, riveted railway bridges was considered by Imam et al. [19,20]. Their research was extended by including uncertainty in both material and loading in the finite element models (FEM) of riveted bridge connections [21, 22].

NCHRP Report 721 [23] indicates that a larger amount of uncertainty is involved in bridge fatigue evaluations as compared to bridge strength evaluations or load ratings. The sources of uncertainty in the fatigue evaluation process include the scattered nature of the S–N curves, variable loads including significant site-to-site variations [24], and approximations in structural analysis or load effect estimation. An important advantage of the existing bridge safety verification and fatigue design of a new bridge is the possibility of in-situ monitoring to determine the real "action effects" in structural elements [25–27]. The inherent uncertainties can be reduced using more refined analyses and field measurements that better define the stress range at the details in question [23]. Fatigue evaluation supported by results of the experimental vibration tests provided information on actual loads acting on the structure and enabled refinement of the theoretical load models of the design codes [28]. "The data can be used for refining the structural analysis and the fatigue assessment as far as they are representative of the operating conditions over the bridge life" [29]. However, it may not always be possible to obtain data from monitoring directly in the cross-section determinant for safety verification; therefore, structural analysis is thus needed to "translate" data from monitoring to sections determinant for the structural safety verification [24].

This paper presents a comparison of fatigue estimation using Eurocode, AREMA, and the probabilistic method that uses newly developed fatigue resistance based on data collected specifically from riveted girders [2]. All three methods are demonstrated on the steel deck plate girder (DPG) railway bridge using data from field monitoring [5]. Using a probabilistic method, the number of cycles or accumulated traffic is estimated in terms of the probability of fatigue crack initiation. A fatigue verification is contingent on the applied load and the fatigue category; which, in turn, depends on member type and its connections. This method provides additional information about the fatigue of a bridge, such as a relationship between the accumulated number of cycles and probability of initial crack detection, that may allow a bridge to be used in service two to three times longer with appropriate inspections [2].

2. Methods for fatigue evaluation

2.1. S–N Curve for fatigue evaluation

The current fatigue evaluation procedures in Eurocodes and North American bridge codes are based on the S–N curves relations that present the number of cycles to failure as a function of constant stress ranges for different categories of details. Design guidelines provide several S–N curves for categories of welded and riveted connections. The current fatigue design S–N curves are based on a two standard deviation shift from the mean values at 2 million cycles that provides a probability of failure of 2.275 percent. Data from full-scale riveted bridge girders were gathered and the statistical investigation was performed to evaluate fatigue resistance of riveted girders [2]. Many aspects of the specimens were considered in the investigation:

1. Material – only steel specimens were considered (wrought iron specimens were excluded). The structural steel used at the time when the components were prefabricated was A7 steel also known as ASTM steel A373, currently this is A36/A36M. While, structural rivet steel is of three types: ASTM A502 grade 1, 2, and 3. Grade 1 and 2 rivets correspond to those formerly made from steel conforming to ASTM A141 and A195, respectively. Grade 3 rivets are made from steel conforming to ASTM A588 [15].
2. Tension due to bending and uniaxial tension.
3. Sub-punched and reamed rivets versus punched rivets.
4. Number of cycles to crack initiation versus the number of cycles to failure.

The investigation revealed that the data follows two trends, and the coefficient of variation of the data points is from 15 to 20 percent. Fig. 2 presents all data collected and used to develop statistical parameters for fatigue resistance and S–N curves from Eurocode and AREMA that are recommended to be used for fatigue evaluation for riveted connections.

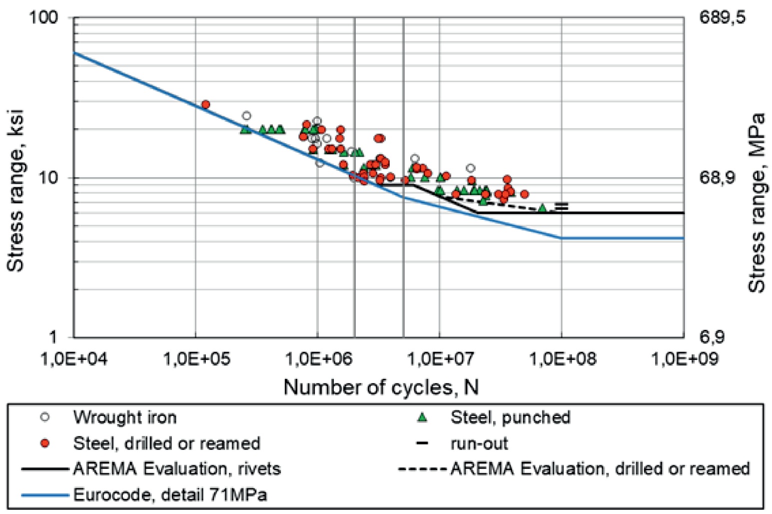

Fig. 2. Comparison of test results from literature review, data for initial crack detection of steel riveted members, and S–N curves from Eurocode and AREMA

In another study of riveted joints, it was found, that the Eurocode Class 71 S–N curves predicted lower fatigue strength compared to experimental observations. However, the tests were performed on small samples that did not reflect the real size of the bridge [30]. For double shear riveted connection, an S–N curve with an inverse slope of four was found to have a good correlation with the experimental data [31]. These research findings will be valuable to consider fatigue in connections of the floor beams and stringer or between the members of truss bridges.

2.2. Fatigue evaluation using AREMA

Bridge fatigue verification is normally first made using theoretical calculations. The quick and simple calculations using basic load rating information are conservative. More detailed calculations, taking full advantage of the AREMA rating provisions, can provide a better estimate. Where actual strain gauge data is available, it provides a more accurate estimate of fatigue verification for a particular structure [7]. Past traffic history is also necessary to determine the remaining safe service of a bridge; that subject will be addressed in further sections. For stress ranges above 62 MPa (9 ksi), AREMA [7] and the American Association of State Highway and Transportation Officials (AASHTO) [32], per the National Steel Bridge Alliance (NSBA), both recommend the same fatigue estimation procedure for riveted spans, which is the standard Category D fatigue (S–N) curve. The corresponding number of cycles can be calculated using Equation 2.1.

$$S_r > 9\,\text{ksi}\ (62\,\text{MPa}) \longrightarrow N = 2,183 \cdot 10^9 \cdot S_r^{-3}. \tag{2.1}$$

Following AREMA guidelines, an equivalent stress range S_r (net section, unit: ksi) can be calculated using the root-mean-cube method ignoring cycles below the fatigue limit of 6 ksi [33]. For optional evaluation of drilled or reamed bridge components (Figure 15-9-12 [7]) where the rivets are tight and rivet holes are smooth, having been correctly drilled or sub-punched and reamed, a further refinement in the allowable stress range is permissible and the number of cycles can be calculated using Equations 2.2 and 2.3.

$$9\,\text{ksi}\ (62\,\text{MPa}) \geq S_r > 7.65\,\text{ksi}\ (53\,\text{MPa}) \longrightarrow N = 4.446 \cdot 10^9 \cdot S_r^{-3} \tag{2.2}$$

$$7.65\,\text{ksi}\ (53\,\text{MPa}) \geq S_r > 6\,\text{ksi}\ (41\,\text{MPa}) \longrightarrow N = 2.465 \cdot 10^{15} \cdot S_r^{-9.5} \tag{2.3}$$

In case, the actual stress cycles can be estimated from traffic records and future estimate traffic, an effective stress range can be determined for the total number of variable stress cycles. The measured number of cycles n_i for each stress range is then used to determine fatigue damage d_i per stress range that can be calculated using Equation 2.4. And by summing up all stress ranges, the total damage D is obtained from Equation 2.5 (if $D = 1.0$ a fatigue failure is supposed to occur).

$$d_i = \frac{n_i}{N_i} \tag{2.4}$$

$$D = \sum_{i=1}^{k} d_i \tag{2.5}$$

2.3. Fatigue evaluation using Eurocode

The Eurocode (EN 1993-1-9 [34]) evaluation is also based on the classification method which employs S–N curves in conjunction with tables of category details. The safety level for the fatigue limit state can be expressed by Equation 2.6.

$$\mu_{\text{fat}} = \frac{\Delta\sigma_C}{\gamma_{Mf}\gamma_{Ff}\Delta\sigma_{E,2}} \geq 1.0 \tag{2.6}$$

where μ_{fat} – fatigue safety level; $\Delta\sigma_C$ – fatigue resistance at $N_C = 2\cdot10^6$ cycles (detail category); $\Delta\sigma_{E,2}$ – equivalent constant amplitude stress range at $2\cdot10^6$ cycles; γ_{Mf} – partial safety factor for fatigue strength $\Delta\sigma_C$; γ_{Ff} – partial safety factor for equivalent constant amplitude stress range $\Delta\sigma_{E,2}$.

Based on Miner's rule and Wöhler curves, an equivalent stress range for stress spectra can be derived. The equivalent stress spectra are obtained by Equation 2.7.

$$\sigma_e = \Delta\sigma_{\max} \sqrt[m]{\sum_{i=1}^{n} \frac{n_i}{n}\left(\frac{\Delta\sigma_i}{\Delta\sigma_{\max}}\right)^m} \tag{2.7}$$

Determination of the remaining fatigue of a structure exposed to a varied stress range can also be obtained by calculating an equivalent stress range. The remaining service life is then determined by comparison of that stress to the valid Wöhler curve (detail category). From S–N fatigue strength curves, Equations 2.8–2.10 are distinguished:

$$\Delta\sigma_R^m \cdot N_R = \Delta\sigma_C^m \cdot 2\cdot10^6 \qquad \text{with} \quad m = 3 \quad \text{for} \;\; N \leq 5\cdot10^6 \tag{2.8}$$

$$\Delta\sigma_R^m \cdot N_R = \Delta\sigma_D^m \cdot 5\cdot10^6 \qquad \text{with} \quad m = 5 \quad \text{for} \;\; 5\cdot10^6 \leq N \leq 10^8 \tag{2.9}$$

$$\Delta\sigma_L = 0.549\Delta\sigma_D \qquad \text{is the cut off limit} \tag{2.10}$$

where:

$\Delta\sigma_C$ – reference value of the fatigue strength at N_C 2 million cycles,
$\Delta\sigma_D$ – fatigue limit for constant amplitude stress ranges at the number of cycles N_D,
$\Delta\sigma_L$ – cut-off limit for stress ranges at the number of cycle N_L,
N_R – design lifetime expressed as a number of cycles related to a constant stress range.

Once the number of cycles related to a constant stress range N_{Ri} is obtained, the measured number of cycles n_i for each stress range calculated using net-section stresses is then used to determine fatigue damage d_i per stress range. And by summing up all stress ranges, the total damage D is obtained. Fatigue category of $\Delta\sigma_C = 71$ MPa (with a constant amplitude fatigue limit of $\Delta\sigma_D = 52$ MPa) is recommended for riveted members.

2.4. Probabilistic method and fatigue resistance parameters

The probabilistic method is employed to account for the variability in the applied load and fatigue resistance. The scattered nature of S–N curves is one of the factors that influence the uncertainty of fatigue verification. In this situation, fatigue resistance should be considered as a random variable (i.e., the coefficient of variation about the mean value is normally distributed). The probability of fatigue crack initiation depends on the selection of values of statistical parameters representing a relevant fatigue category.

Data from full-scale riveted bridge girders were gathered to evaluate the fatigue resistance of riveted details and is presented in Fig. 1. A plot of the selected fatigue test data revealed that the data follows two trends: the data points below a stress range of 69 MPa (10 ksi) have a different distribution than data points above 69 MPa (10 ksi) [2]. The first part of the curve, for stress range above 69 MPa (10 ksi), is taken with a slope of 3, as is common; the second part of the curve, from 69 MPa (10 ksi) to 41 MPa (6 ksi), is assumed to have a slope of 5, similar to Eurocode. The fatigue limit is taken to be 41 MPa (6 ksi), as in most current recommended practices. Details about the data and the process of developing the statistical parameters are described in the previous study [2]. Table 1 presents the statistical parameters of fatigue resistance in SI units.

Table 1. Statistical parameters for riveted members, SI units

Slope	Mean fatigue resistance:	Mean number of cycles	Coefficient of Variation
$m = 3$, $\sigma > 70$ MPa (10 ksi)	95 MPa	$N = \dfrac{\mu_R^3 \cdot 2 \cdot 10^6}{S_{\text{eff}}^3}$	16.5%
$m = 5$, $\sigma \leq 70$ MPa (10 ksi)	70 MPa	$N = \dfrac{\mu_R^5 \cdot 5 \cdot 10^6}{S_{\text{eff}}^5}$	15%

Advanced statistical analyses, such as the probabilistic method, are the only way to the evaluation of bridge fatigue with consideration of the uncertainties involved in the load and resistance. An important step in applying the probability method is to define a limit state function. The limit state function for fatigue of steel railway bridges can be expressed in terms of the accumulated fatigue ratio, as seen in Equation 2.11 [37].

$$D = \frac{\sqrt[3]{\sum\limits_i S_{Qi}^3 \cdot N_{Qi}}}{\sqrt[3]{\sum\limits_i S_{Ri}^3 \cdot N_{Ri}}} \leq 1 \tag{2.11}$$

Equivalent stress for special conditions can lead to a fatigue parameter of $(S_i^3 N)^{(1/3)}$. This parameter is calculated for resistance, $(S_{Ri}^3 N_{Ri})^{(1/3)}$, using the S–N relationship and a constant coefficient A, as per the statistics presented in Table 1. Also, a fatigue parameter can be calculated for a load, $(S_{Qi}^3 N_{Qi})^{(1/3)}$, using stress histories and variations related to the load. Therefore, the accumulated fatigue ratio is a ratio of load Q and resistance R (Equation 2.12, where S_{Ri} and N_{Ri} are the equivalent stress and number of cycles representing the design criteria; S_{Qi} and N_{Qi} are the equivalent stress and number of cycles due to a live load). In a case, when the cumulative distribution function (CDF) of the load is constant in time, the values of $S_{Qi} = S_{Ri}$ and the ratio of N_{Ri}/N_{Qi} is constant for all "i". then D depends only on the ratio of N_R/N_Q. Therefore, for a given CDF of the service load, resistance and load can be represented by the number of load cycles to fatigue crack initiation, and the number of cycles applied, respectively.

Once, the statistical parameters of load and resistance are quantified, the reliability index can be calculated, which later can be converted to the probability of crack initiation. Based on the initial statistical analysis, both Q and R can be considered as normal variables. Therefore, the basic statistical parameters required for reliability analysis are μ_R and μ_Q – mean values of resistance and load respectively; and σ_R and σ_Q – standard deviations; and coefficient of variation, V (ratio of standard deviation to mean value). For special cases, such as a case of two normally distributed, uncorrelated random variables, Q and R, the reliability index is given by Equation 2.12 [38].

$$\beta = \frac{\left(\mu_R - \mu_Q\right)}{\sqrt{\sigma_R^2 + \sigma_Q^2}} \tag{2.12}$$

The accumulated fatigue ratio is a function of two parameters: effective stress, S, and a number of cycles, N. However, when analyzing a particular detail in a bridge, the equivalent stresses are on the same level for a given load type. The variability in stresses is only related to the axle load, but the major time variation is involved in N, a number of cycles to failure. This is true with the assumption that the train will continue to operate with the same car weights.

3. Case study

3.1. The spans at Facility for Accelerated Service Testing (FAST)

The testing had been conducted at the Facility for Accelerated Service Testing (FAST), located at the Transportation Technology Center (TTC) in Pueblo, CO, USA. TTC's High Tonnage Loop (HTL) at FAST is 2.7 miles (4.3 km) and is well-known in the railway industry as the primary place for testing and evaluation of track components, from rails and sleepers to ballast and subgrade [35]. The bridges at FAST carry approximately 136 MGTonnes (150 MGTons) per year of heavy axle load (HAL) traffic. TTCI was using these bridges to investigate improved safe service life estimates for common steel railway bridge spans.

The investigated railway bridge has two riveted steel DPG spans with open decks (Fig. 3). It is located on a 5-degree curve and is super elevated by 100 millimeters (4 inches) [5]. The two short steel DPG bridge spans on West Steel Bridge were donated by two different railways and installed in December 2014 [5]. A 7.3-meter (24-foot) span was built in 1913 and was installed without any changes. While, a 10-meter (33-foot) span constructed in 1904 was shortened by ~180 millimeters (7 inches) at each end to fit the existing opening; making it a 9.75-meter (32-foot) span. The dimensions of the cross-sections are summarized in Table 2.

Both spans are being overloaded by the HAL train at FAST. However, up to date, both spans have performed well; no maintenance has been required and no defects have been noted during the operation of HAL traffic. The considered case study was previously described in more detail in the previous publication [35].

Fig. 3. The West Steel Bridge

Table 2. Characteristic of a built-up section of main girders

<table>
<tr><td rowspan="7">Built-up section of the main girder of 9.75-meter span</td><td>Top partial length cover plate 381 × 11 × 6807 mm</td><td rowspan="7">$S_{x,\text{gross}} = 859$ in^3
$S_{x,\text{net}} = 737$ in^3
$\dfrac{S_{x,\text{gross}}}{S_{x,\text{net}}} = 1.164$</td></tr>
<tr><td>Top full-length cover plate 381 × 9.5 × 9700 mm</td></tr>
<tr><td>Top flange angles 152 × 152 × 13 × 9700 mm</td></tr>
<tr><td>Web 927 × 9.5 × 9700 mm</td></tr>
<tr><td>Bottom flange angles 152 × 152 × 13 × 9700 mm</td></tr>
<tr><td>Bottom full-length cover plate 381 × 9.5 × 9700 mm</td></tr>
<tr><td>Bottom partial length cover plate 381 × 11 × 6807 mm</td></tr>
<tr><td rowspan="7">Built-up section of the main girder of 7.3-meter span</td><td>Top partial length cover plate 356 × 11 × 4369 mm</td><td rowspan="7">$S_{x,\text{gross}} = 728$ in^3
$S_{x,\text{net}} = 612$ in^3
$\dfrac{S_{x,\text{gross}}}{S_{x,\text{net}}} = 1.189$</td></tr>
<tr><td>Top full-length cover plate 356 × 11 × 7315 mm</td></tr>
<tr><td>Top flange angles 152 × 152 × 16 × 7315 mm</td></tr>
<tr><td>Web 927 × 9.5 × 7315 mm</td></tr>
<tr><td>Bottom flange angles 152 × 152 × 16 × 7315 mm</td></tr>
<tr><td>Bottom full-length cover plate 356 × 11 × 7315 mm</td></tr>
<tr><td>Bottom partial length cover plate 356 × 11 × 4369 mm</td></tr>
</table>

3.2. Data collection and span load history

The strain gages and string potentiometers are located at the bottom cover plates at mid-spans on all main girders of the West Steel Bridge at FAST that has an automated data collection system triggered when the train approaches the bridge. Data is collected and recorded for every single pass of a train [35]. Train operations at FAST include a train of primarily 143 tonnes gross rail load (GRL) cars – approximately 10 percent heavier than the maximum interchange standard of 130 tonnes GRL. Train length is up to 110 cars. Normal train operations at FAST are at 64 km/h (40 mph). Both spans are being overloaded by the HAL train at FAST: the 7.3-meter span is overload by 7 percent and the 9.75-meter span is overloaded by 33 percent. The overload includes the effects of unbalanced superelevation [36]. Both spans unload completely (live load stress goes to zero) under the center of each car. This is expected as the span lengths are less than the inside axle spacing on the cars of ~10.5 meters (34.5 feet). Thus, there is a brief period beneath each car when there are no axles on the span. Since fatigue is governed by the stress range or magnitude of the stress cycles, these short spans can be more susceptible to fatigue as compared to longer spans that do not experience full unloading as a train traverse.

For fatigue evaluation, the following steps are taken:

1. The cycles are counted using a rain flow cycle counting method. The histograms are presented in Fig. 4.

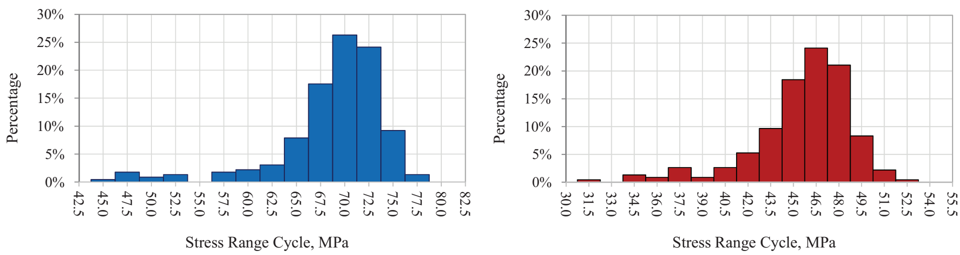

Fig. 4. Stress range cycles for the FAST 9.75-meter (32-foot) steel span (left) and 7.3-meter (24-foot) span (right) (1 MPa = 0.145 ksi)

2. An equivalent stress range is calculated using the root-mean-cube method for slope 3 or the modified method for other slopes. The average equivalent stress ranges for the south girders under the high rail are 7.3-meter span – 44.8 MPa (6.5 ksi) and 9.75-meter span – 68 MPa (9.85 ksi).
3. Calculate statistical parameters of load effect distribution. Variations in the equivalent stresses for these girders are from 4 percent to 7 percent. The bridges are tested in controlled conditions; therefore, the coefficient of variations are low.

Additional information about past load history is necessary to use fatigue verification properly. The 9.75-meter span accumulated 816 MGTonnes of 119-tonne car traffic and 726 MGTonnes of 130-tonne car traffic in revenue service. The stress levels were 49 MPa and 53 MPa respectively. The FAST train loading on the high rail girder produces stresses of 68 MPa. The FAST tonnage accumulated is about 432 MGTonnes (476 MGT) which corresponds to 3.0 million cycles. The 7.3-meter span accumulated about 883 MGTonnes during the revenue service operation, but that corresponds to less than 1 million accumulative cycles (888,437). At FAST, the total tonnage accumulated is about 432 MGTonnes (476 MGT) which corresponds to 3.0 million cycles at a stress of 44.9 MPa [7].

4. Results of fatigue evaluation

4.1. Fatigue verification using AREMA

As the locations of measurements are generally not identical with the cross-sections of verification, measured strains were translated to the relevant verification cross-section utilizing factors that represent gross to net section ratio. Table 3 presents fatigue verification for 7.3-meter

(24-foot) using AREMA. The total fatigue damage ratio is 0.427. To reach a damage ratio of 1.0 additional 5.5 million cycles at a stress range (net section) of 7.47 ksi (53.4 MPa) are allowed.

Table 3. AREMA fatigue evaluation for 7.3-meter (24-foot) span and fatigue damage

Measured Stress range (gross section)	Stress range (net section) S_i, ksi (MPa)	Accumulated Cycles up to date, n_i	Maximum number of stress cycles for each of the stress range values, N_i	Fatigue damage ratio d_i
9.33 (64.3)	11.09 (76.5)	172,325	1,599,054	0.108
6.15 (42.4)	7.31 (50.4)	759,980	15,250,206	0.005
6.51 (44.9)	7.47 (53.4)	3,015,042	9,586,960	0.314

Table 4 presents fatigue verification for 9.75-meter (32-foot) using AREMA. The total fatigue damage ratio is 5.6 times larger than the allowed 1.0. This span has performed well with no maintenance required and no indication of fatigue damage. It is still safely used at FAST as reported by TTCI in the latest publication [2].

Table 4. AREMA fatigue evaluation for 9.75-meter (32-foot) span and fatigue

Measured Stress range (gross section)	Stress range (net section) S_i, ksi (MPa)	Accumulated Cycles up to date, n_i	Maximum number of stress cycles for each of the stress range values, N_i	Fatigue damage ratio d_i
7.1 (49)	8.26 (57.0)	6,628,369	3,867,406	1.714
7.7 (53)	8.99 (61.7)	5,431,831	3,008,451	1.806
9.85 (68)	11.47 (79.2)	3,015,042	1,448,392	2.082

4.2. Fatigue verification using Eurocode

The example fatigue verification using Eurocode is calculated for riveted built-up sections under flexural bending due to traffic from in-situ measurements. Fatigue category of $\Delta\sigma_C =$ 71 MPa (with a constant amplitude fatigue limit of $\Delta\sigma_D = 52$ MPa) is used and the number of cycles related to a constant stress range is calculated using Equations (2.8) and (2.9)

$$N_{Ri} = \frac{\Delta\sigma_C^m \cdot 2 \cdot 10^6}{\Delta\sigma_{Ri}^m} = \frac{71^3 \cdot 2 \cdot 10^6}{\Delta\sigma_{Ri}^3}$$

The measured number of cycles n_i for each stress range is then used to determine fatigue damage di per stress range and by summing up all stress ranges, the total damage D is obtained. Table 5 presents fatigue verification for 7.3-meter (24-foot) using Eurocode. The total fatigue damage ratio is 0.762. To reach a damage ratio of 1.0 additional 1.1 million cycles at a stress range (net section) of 53.4 MPa (7.47 ksi) are allowed. In this case, the fatigue verification using Eurocode is more conservative than using AREMA.

Table 5. Eurocode fatigue evaluation for 7.3-meter (24-foot) span and fatigue damage

Measured Stress range (gross section)	Stress range (net section) S_i, ksi (MPa)	Accumulated Cycles up to date, n_i	Maximum number of stress cycles for each of the stress range values, N_{Ri}	Fatigue damage ratio d_i
9.33 (64.3)	11.09 (76.5)	172,325	1,601,867	0.108
6.15 (42.4)	7.31 (50.4)	759,980	5,586,784	0.014
6.51 (44.9)	7.47 (53.4)	3,015,042	4,704,576	0.641

Table 6 presents fatigue verification for 9.75-meter (32-foot) using Eurocode. The total fatigue damage ratio is 5.6 times larger than the allowed 1.0. The fatigue verification using Eurocode and AREMA is very similar for this case.

Table 6. Eurocode fatigue evaluation for 9.75-meter (32-foot) span – revenue

Measured Stress range (gross section)	Stress range (net section) S_i, ksi (MPa)	Accumulated Cycles up to date, n_i	Maximum number of stress cycles for each of the stress range values, N_i	Fatigue damage ratio d_i
7.1 (49)	8.26 (57.0)	6,628,369	3,857,961	1.718
7.7 (53)	8.99 (61.7)	5,431,831	3,048,727	1.782
9.85 (68)	11.47 (79.2)	3,015,042	1,443,509	2.089

4.3. Fatigue evaluation using probability method

Example calculations are presented using load histories and fatigue resistance from Table 1. For stresses less than 69 MPa (10 ksi) slope $m = 5$ resistance parameters should be used: $\mu_R = 225$, $\sigma_R = 33$. For the stresses from the past operation, it is assumed that the COV is 10 percent.

Example of 9.75-meter (32-foot) span:

At 6.8 million cycles, equivalent stresses are 49 MPa (7.1 ksi), therefore:

$$\mu_Q = \sqrt[5]{\frac{\sum_i S_{Qi}^5 \cdot N_{Qi}}{5 \cdot 10^6}} = \sqrt[5]{\frac{49^5 \cdot 6.8 \cdot 10^6}{5 \cdot 10^6}} = 52.1 \quad \text{and} \quad \sigma_Q = \mathrm{COV}_Q \cdot \mu_Q = 0.1 \cdot 52.1 = 5.21$$

$$\beta = \frac{70 - 52.1}{\sqrt{10.5^2 + 5.21^2}} = 1.53$$

The probability is calculated from β using the standard normal cumulative distribution function (Microsoft® Excel command NORMDIST).

$$P_f = \Phi(-\beta) = \Phi(-1.53) = 0.063 = 6.3\%$$

At 12.0 million cycles, the equivalent stress is 51 MPa (7.4 ksi) (calculated from 6.6 million cycles at 49 MPa (7.1 ksi) and 5.4 million cycles at 53 MPa (7.7 ksi) using slope 5:

$$\sqrt[5]{\sum_i \left(S_{Qi}^5 \cdot N_{Qi}\right) \Big/ \sum_i N_{Qi}} = \sqrt[5]{(49^5 \cdot 6.6 \cdot 10^6 + 53^5 \cdot 5.4 \cdot 10^6) \,/\, (6.6 \cdot 10^6 + 5.4 \cdot 10^6)} = 51$$

therefore:

$$\mu_Q = \sqrt[5]{\frac{\sum_i S_{Qi}^5 \cdot N_{Qi}}{5 \cdot 10^6}} = \sqrt[5]{\frac{51^5 \cdot 12 \cdot 10^6}{5 \cdot 10^6}} = 60.8 \quad \text{and} \quad \sigma_Q = \mathrm{COV}_Q \cdot \mu_Q = 0.1 \cdot 60.8 = 6.08$$

$$\beta = \frac{70 - 60.8}{\sqrt{10.5^2 + 6.08^2}} = 0.762 \quad \rightarrow \quad P_f = \Phi(-\beta) = \Phi(-0.762) = 0.22 = 22\%$$

At 15 million cycles, the equivalent stresses are 56.5 MPa (8.2 ksi) calculated from 12 million cycles at 51 MPa (7.4 ksi) and 3.0 million cycles at 68 MPa (9.85 ksi) using slope 5. The reliability index for this case was calculated at the level of 0.06. Therefore, at 15 million cycles, the probability of crack initiation is around 47.8 % (Fig. 5, on the left). The bridge experiences maximum stress ranges below 69 MPa (10 ksi); therefore, it can be compared to a slope of 5 on the S–N curve. With this assumption, the bridge span has about a 50 percent probability of fatigue crack initiation with the current 15 million cycles. When comparing the fatigue predictions of the bridge to slope 3, the bridge has about 60 percent probability of fatigue crack initiation, and the probability of crack initiation is rising faster. It appears to be appropriate to use slope 5 of new fatigue resistance statistics. That leads to the conclusion that the bridge can be used up to 22 million cycles with the prediction of fatigue crack initiation around 75 percent.

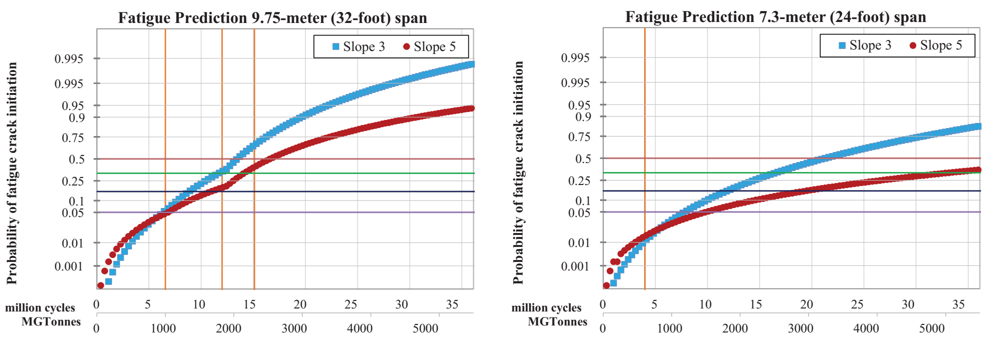

Fig. 5. Fatigue predictions for considered span using the probabilistic method

Similarly, the calculations were carried for the 7.3-meter (24-foot) span and the results are presented in Fig. 5 (on the right). The results show that the bridge span has less than a 1 percent probability of fatigue crack initiation (detection) with the current accumulated cycles around 4 million. The Minimum Fatigue Life with a 5 percent probability of crack initiation and reliability index of 1.64 will be reached around 10 million cycles using the probabilistic method.

The probabilistic method with slope 3 is more conservative when looking at small stress ranges and low probability of crack initiation (detection). However, a large increase in fatigue predictions is noticed when the span is considered using the proposed new statistical parameters for riveted details with a higher number of cycles. The slope of the red-dotted line in Fig. 5 (on the right) decreases after 10 million cycles. This can be an indication that the span has close to infinite fatigue life. This can be true since the equivalent stress for the span under current operating conditions is only 6.5 ksi (44.8 MPa). This scenario doubles or triples the estimated span safe service for the same probability of crack initiation (detection) when compared to the scenario of fatigue verification using current codes for the entire bridge.

5. Discussion and conclusions

Fatigue verification of existing riveted steel bridges using current Eurocode and AREMA recommendations provide general methods from basic evaluation to more complex and sophisticated analysis. The methods that employ the monitored value improve fatigue evaluation; however, they are still based on conservative limits of 95 percent of confidence. From the two examples presented in this paper, it was observed that the Eurocode is more conservative for the stress range below 48 MPa (7 ksi), while for the higher stress rangest the fatigue verification is similar for both standards. The fatigue safety of the 9.75-meter span considered in this paper already has been exceeded, according to the AREMA and Eurocode calculations. However, the span is in operation with no maintenance required, no defects noted and has accumulated additional cycles due to heavy axle load. This example confirms that the fatigue verification evaluated using current methods is too conservative. The examples show in this paper and examples by other researchers (e.g. [24]) confirm that verification of structural performance does not depend on the age of a structure but their current technical condition and the live load spectra that the bridge is and will be exposed to.

For riveted structures where the members are fabricated from multiple elements, the immediate consequences of fatigue cracking may not be as serious as in welded structures. The riveted built-up members and connections have internal redundancy. Therefore, if one element fails there is normally sufficient capacity and redundancy for the force to be redistributed. The members will usually survive long enough for the crack to be detected by routine inspection thereby permitting corrective action before more serious damage develops [7].

The probability of failure can provide the most versatile estimate of the remaining safe service life of a span that depends on the fatigue category, material properties, and applied load. During the service life of a bridge, the accumulated fatigue is increasing in time at different rates, depending on tonnage per year and train type. All these factors must be specified to obtain accurate results from the reliability analysis. Using a probabilistic method, the number of cycles of accumulated traffic is estimated in terms of the probability of fatigue crack initiation (detection). The reliability analysis can be used for estimating the remaining service life of a bridge with different levels of safety.

It is recommended that a probabilistic method be used for steel riveted spans when a higher probability of crack initiation is accepted, understanding that inspection efforts must be increased accordingly. In particular, it is advised that the method be used for steel spans that have exceeded their fatigue safety according to conventional calculations but show no signs of deterioration, and fatigue cracks are not present. The method can be also applied to more complex structures such as through plate girder bridges and trusses. The connection between stringer and floor beam acquires a certain degree of rotational stiffness and develops stress concentration due to bending moment [39] – these connections should be verified for fatigue using refine fatigue resistance that includes a complex state of stress due to shear and flexural bending. However, the material parameters and fatigue resistance of structural steel is needed, especially from old bridges where the steel properties are unknown. The S–N relation, developed and used in this study, was determined based on the data from bridges located in the U.S. and made from ASTM steel A373 (A36/A36M) and maybe not suitable for fatigue behavior prediction of old metallic bridges in Europe. Further research to evaluate fatigue prediction of riveted bridges in Europe using the probabilistic method is recommended.

References

[1] J. Olofsson et al., “Assessment of European Railway Bridges for Future Traffic Demands and Longer Lives – EC Project “Sustainable Bridges”. Journal of Structure and Infrastructure Engineering, vol.1, no. 2, pp. 93–100, 2005, DOI: 10.1080/15732470412331289396.

[2] A.M. Rakoczy, D. Otter, and S. Dick, “Railroad bridge fatigue life estimation using the probabilistic method and new fatigue resistance for riveted details”. Structure and Infrastructure Engineering, Maintenance, Management, Life-Cycle Design and Performance, vol. 16, no. 3, pp. 381–393. 2020, DOI: 10.1080/15732479.2019.1663220.

[3] F. Moreu, J. LaFave, “Current Research Topics: Railroad Bridges And Structural Engineering”. NSEL Report Series Report No. NSEL-032 October 2012. http://hdl.handle.net/2142/34749.

[4] H. Isami, “Plate-Girder Construction”. Publisher: BiblioBazaar. 2008.

[5] D. Otter, S. Dick, and A.M. Rakoczy, “Update on FAST Bridge Research and Testing”. In Proc. AREMA 2017 Annual Conference. Indianapolis, Indiana USA. September 2017.

[6] R.A.P. Sweeney, “Resistance and Loading for Steel Bridge Fatigue Life Evaluation”. Proceedings of AREMA Conference. Minneapolis MN, USA, 2015.

[7] American Railway Engineering and Maintenance of Way Association, Manual for Railway Engineering AREMA. Chapter 15 – Steel Structures, Lanham, Maryland, 2020.

[8] Comité Européen de Normalisation, EN 1990. Eurocode: Basic design rules of structures, Warsaw 2004.

[9] Comité Européen de Normalisation, EN 1991-2. Eurocode 1: Actions on structures – Part 2: Traffic loads on bridges, Warsaw 2007.

[10] H. Zobel, T. Alkhafaji, and M. Wróbel, “Metoda określanie trwałości mostów drogowych”. Inżynieria i Budownictwo, no. 11, pp. 582–587, 2017.

[11] T. Siwowski, “Fatigue assessment of existing riveted truss bridges: case study”. Bulletin of The Polish Academy Of Sciences -Technical Sciences, vol. 63, no. 1, 2015, DOI: 10.1515/bpasts-2015-0014.

[12] E. Bruhwiler, I.F.C .Smith, and M. Hirt, “Fatigue and Fracture of Riveted Bridge Members”. Journal of the Structural Engineering vol. 116, no. 1, pp. 198–213, 1990, DOI: 10.1061/(ASCE)0733-9445(1990)116:1(198).

[13] A. Pipinato, C. Pellegrino, O.S. Bursi, C. Modena,, “High-cycle Fatigue Behavior of Riveted Connections for Railway Metal Bridges”. Journal of Constructional Steel Research, vol. 65, no. 12, pp. 2167–2175, 2009. DOI: 10.1016/j.jcsr.2009.06.019.

[14] M. Al-Emrani, “Fatigue Performance of Stringer-to-Floor-Beam Connections in Riveted Railway Bridges”. J. Bridge Eng., vol. 10, no. 2, pp. 179–185, 2005, DOI: 10.1061/(ASCE)1084-0702(2005)10:2(179).

[15] Y. Zhou, “Assessment of Bridge Remaining Fatigue Life through Field Strain Measurement”. Journal of Bridge Engineering, vol. 11, no. 6, November 2006, DOI: 10.1061/(ASCE)10840702(2006)11:6(737).

[16] P.M. Kunz and M.A. Hirt, “Evaluation of the Remaining Fatigue Life of Steel Bridges”. Fourth International Conference on Short and Medium Span Bridges, pp. 1219–1230. Halifax, Nova Scotia, Canada. 1994.

[17] E. Brühwiler and P. Kunz, "Remaining Fatigue Life of a Riveted Railway Bridge". Proc. IABSE Colloquium: Remaining Structural Capacity, pp. 375–383. Copenhagen, Denmark. 1993.

[18] D.H. Tobias and D.A. Foutch, "Reliability-Based Method for Fatigue Evaluation of Railway Bridges". Journal of Bridge Engineering, vol. 2, no. 2, pp. 53–60, 1997, DOI: 10.1061/(ASCE)1084-0702(1997)2:2(53).

[19] B. Imam, T.D. Righiniotis, and M.K. Chryssanthopoulos, "Fatigue Assessment of Riveted Railway Bridges". International Journal Steel Structures (KSSC), vol. 5, no.5, pp. 485–494, 2005.

[20] B. Imam, et al.,"Analytical Fatigue Assessment of a Typical Riveted UK Rail Bridge". Proceedings of the Institution of Civil Engineers (ICE) – Bridge Engineering, vol. 159, no.3, pp. 105–116, 2006, DOI: 10.1680/bren.2006.159.3.105.

[21] B.M., Imam, T.D. Righiniotis, and M.K. Chryssanthopoulos, "Numerical Modeling of Riveted Railway Bridge Connections for Fatigue Evaluation". Engineering Structures, vol. 29, no. 11, pp. 3071–3081, 2007, DOI: 10.1016/j.engstruct.2007.02.011.

[22] B.M., Imam, T.D. Righiniotis, and M.K. Chryssanthopoulos, "Probabilistic Fatigue Evaluation of Riveted Railway Bridges". Journal of Bridge Engineering (ASCE), vol. 13 no. 3, pp. 237–244, 2008, DOI: 10.1061/(ASCE)1084-0702(2008)13:3(237).

[23] M.D., Bowman, et al., "Fatigue Evaluation of Steel Bridges". NCHRP Report 721, Transportation Research Board, Washington D.C., USA. 2012, DOI: 10.17226/22774.

[24] E. Brühwiler, "Extending the Fatigue Life of Riveted Bridges Using Data From Long-Term Monitoring". Advanced Steel Construction, vol. 11, pp. 283–293, 2015, DOI: 10.18057/IJASC.2015.11.3.3.

[25] M. Treacy and E. Brühwiler, "Fatigue Loading Estimation for Road Bridges Using Long Term WIM Monitoring". Advances in Safety, Reliability and Risk Management – Proceedings of the European Safety and Reliability Conference, ESREL 2011, Troyes, France, 2011.

[26] M. Kużawa, T. Kamiński, J. Bień, "Fatigue Assessment Procedure for Old Riveted Road Bridges". Archives of Civil and Mechanical Engineering, vol. 18, pp.1259–1274, 2018, DOI: 10.1016/j.acme.2018.03.005.

[27] K.A. Flanigan, J.P. Lynch, and M. Ettouney "Probabilistic Fatigue Assessment of Monitored Railroad Bridge Components Using Long-Term Response Data in A Reliability Framework". Structural Health Monitoring vol. 19, no. 6, pp. 2122–2142, 2020, DOI: 10.1177/1475921720915712.

[28] B. Akesson, "Fatigue Life of Riveted Steel Bridges". CRC Press/Balkema, London, 2010.

[29] C. Cremona, et al., "Improved Assessment Methods for Static and Fatigue Resistance of Old Metallic Railway Bridges". Journal of Bridge Engineering, ASCE, November 2013, DOI: 10.1061/(ASCE)BE.1943-5592.0000466.

[30] A.L.L., Silva et al., "Fatigue Strength Assessment of Riveted Details in Railway Metallic Bridges". Engineering Failure Analysis, vol. 121, 2021, DOI: 10.1016/j.engfailanal.2020.105120.

[31] B. Pedrosa et al., "Reliability of Fatigue Strength Curves for Riveted Connections Using Normal and Weibull Distribution Functions". ASCE-ASME J. Risk Uncertain Eng.. Syst Part A Civ Eng., vol. 6, 2020, DOI: 10.1061/AJRUA6.0001081.

[32] American Association of State Highway and Transportation Officials (AASHTO) 2017. Load and Resistance Factor Design (LRFD). Bridge Design Specification, 8th Edition.

[33] J.W. Fisher, G.L. Kulak, and I.F.C. Smith, "A Fatigue Primer for Structural Engineers". National Steel Bridge Alliance, 1998. https://www.aisc.org/globalassets/nsba/technical-documents/a-fatigure-primer-for-structural-engineers.pdf.

[34] Comité Européen de Normalisation, EN 1993-1-9, 2005. Design of Steel Structures, Part 1–9: Fatigue, European Committee for Standardization.

[35] A.M. Rakoczy and D. Otter, "Highlights of Railway Bridge Research and Testing by TTCI". 64th Scientific Conference Krynica Zdrój, Poland, 16–20.09.2018.

[36] A.M. Rakoczy and D. Otter, "Can 100-year-old Steel Railroad Bridges Continue To Be Used In Service?". IABSE Congress, New York City, N.Y., September 2019.

[37] A.M. Rakoczy, A. S. Nowak, and S. Dick, "Fatigue Reliability Model for Steel Railway Bridges". Structure and Infrastructure Engineering, Maintenance, Management, Life-Cycle Design, and Performance, vol. 12, no.12, pp. 1602–1613, 2016, DOI: 10.1080/15732479.2016.1153664.

[38] C.A. Cornell, "Bounds on the Reliability of Structural Systems". Journal of Structural Division, ASCE, vol. 93, no. 1, pp. 171–200, 1967, DOI: 10.1061/JSDEAG.0001577.

[39] A.M. Rakoczy and A.S. Nowak, "Reliability-Based Strength Limit State for Steel Railway Bridge". Structure and Infrastructure Engineering, published online, pp. 1–14, September 2013, DOI: 10.1080/15732479.2013.807291.

Weryfikacja poziomu zmęczenia stalowych, nitowanych mostów i wiaduktów kolejowych metodą probabilistyczną i normowymi krzywymi S–N

Słowa kluczowe: mosty kolejowe; nitowane konstrukcje stalowe; pomierzone odkształcenia; obciążenia cykliczne; bezpieczeństwo zmęczeniowe; pozostały bezpieczny okres użytkowania

Streszczenie:

Obecne procedury oceny zmęczenia w europejskich i amerykańskich normach mostowych nie uwzględniają stopnia niepewności w modelach obciążenia i nośności konstrukcji. Jednak zmienność obciążenia cyklicznego i zmienność nośności wynikająca z właściwości materiału i ich degradacji, mają istotny wpływ na weryfikację bezpieczeństwa z uwagi na zmęczenie konstrukcji. Ocena zmęczenia zależy od skumulowanych cykli obciążenia i kategorii zmęczeniowej dla detalu konstrukcyjnego; co z kolei zależy od typu elementu i jego połączeń. Ocena bezpieczeństwa konstrukcji może być przeprowadzona dokładniej przy użyciu metody probabilistycznej, która pozwala na określenie przewidywanego zmęczenia za pomocą prawdopodobieństwa powstania pęknięcia. Ta metoda dostarcza więcej informacji o oczekiwanej przydatności elementu konstrukcyjnego do dalszej eksploatacji; dzięki temu konstrukcja może być użytkowana przez znacznie dłuższy czas. W artykule przedstawiono porównanie oceny zmęczenia z wykorzystaniem Eurokodu, normy amerykańskiej – AREMA oraz nowego podejścia wykorzystującego metodę probabilistyczną. Metody te zademonstrowano na nitowanych, stalowych dźwigarach mostów kolejowych (DPG) z wykorzystaniem danych z monitoringu terenowego.

Dane inwentaryzacyjne w Europie z 2005 roku wskazują ponad 220 000 obiektów kolejowych – ponad 35 procent tych mostów i wiaduktów ma więcej niż 100 lat, a tylko 11 procent jest eksploatowanych krócej niż 10 lat. Dominują krótkie przęsła, 62 procent ma 10 metrów lub mniej, a tylko 5 procent ma rozpiętość większą niż 40 metrów [1]. W Ameryce Północnej ponad 50 procent mostów kolejowych z blachownicami stalowymi (DPG) (14 000 przęseł), obecnie eksploatowanych, ma ponad 100 lat, a najstarsze mosty mają blisko 150 lat [2]. W związku z tym rośnie potrzeba opracowania skutecznych procedur oceny stanu technicznego i prognozowania przydatności do dalszej eksploatacji starzejących się konstrukcji mostowych.

W minionej dekadzie kilka nitowanych stalowych przęseł mostów kolejowych DPG zostało przetestowanych i przeanalizowanych pod kątem wytrzymałości zmęczeniowej i bezpiecznej eksploatacji w ramach programu badawczego sponsorowanego przez Association of American Railroads (AAR) [5]. Wyniki badań potwierdziły, że uproszczone obliczenia i zachowawcze założenia prowadzą do znacznego obniżenia szacowanego bezpieczeństwa konstrukcji. Obecne metody oceny zmęczenia zostały opracowane na podstawie niskiego prawdopodobieństwo zmęczenia, co oznacza, że nawet jeśli most osiągnie granicę zmęczenia, konstrukcja prawdopodobnie będzie zdatna do dalszej eksploatacji pod warunkiem częstszych inspekcji [6]. American Railway Engineering and Maintenance of Way Association (AREMA) Manual for Railway Engineering, rozdział 15, zawiera rekomendacje oceny zmęczenia opartą na krzywych S–N opracowanych przy użyciu 95-procentowego poziomu ufności dla 97,5 procent przeżywalności zastosowanej do danych testowych wykonanych na próbkach w pełnej skali [7]. Również w normach europejskich [8, 9] trwałość mostu określa się najczęściej z poziomem ufności równym 95 procent. Dlatego też, gdy nośność osiągnie granicę, uszkodzenia mogą wystąpić w 5 procent elementów konstrukcyjnych mostu, np. pęknięcia w złączach, nitach, śrubach sprężające i pęknięcia w płycie betonowej itp. [10]. Jeśli jednak ocena zmęczeniowa wykazała z dużym prawdopodobieństwem, że inicjacja i propagacja pęknięć zmęczeniowych może mieć miejsce w niektórych krytycznych elementach rzeczywistej konstrukcji, stanowi to duże ryzyko zawalenia się obiektu co zagraża bezpieczeństwu jego użytkowników [11].

Weryfikacja zmęczenia istniejących nitowanych mostów stalowych przy użyciu aktualnych zaleceń Eurokodu i AREMA opierają się na podobnych krzywych S–N, które przedstawiają liczbę cykli do zniszczenia w funkcji stałych zakresów naprężeń dla różnych kategorii detali. Na podstawie dwóch przykładów przedstawionych w tym artykule zaobserwowano, że Eurokod jest bardziej konserwatywny dla zakresu naprężeń poniżej 48 MPa (7 ksi), podczas gdy dla wyższych zakresów naprężeń weryfikacja zmęczenia jest podobna dla obu norm.

W przypadku konstrukcji nitowanych, w których dźwigary są zbudowane z wielu elementów, bezpośrednie konsekwencje pękania zmęczeniowego mogą nie być tak poważne, jak w przypadku konstrukcji spawanych. Nitowane blachownice i połączenia mają większą niezawodność wynikającą z nadmiarowości czyli równoległego systemu wielu elementów. Dlatego też, jeśli jeden element ulegnie awarii, zwykle nośność i nadmiarowość są wystarczające do redystrybucji sił wewnętrznych. Element z zainicjowanym pęknięciem zwykle może utrzymać stateczność wystarczająco długo, do momentu wykrycia pęknięcia podczas rutynowej inspekcji, umożliwiając tym samym podjęcie działań naprawczych, zanim rozwiną się poważniejsze uszkodzenia. Jeżeli nie ma konieczności podjęcia natychmiastowych działań naprawczych, prawdopodobny czas między pierwszym wykrywalnym pęknięciem a niekontrolowaną propagacją powinien być uwzględniony przy ustalaniu częstotliwości inspekcji [7].

Prawdopodobieństwo uszkodzenia może dostarczyć bardziej kompleksowe oszacowanie dalszego bezpiecznego okresu użytkowania przęsła, który zależy od kategorii zmęczeniowej i obciążenia eksploatacyjnego dla różnych poziomów bezpieczeństwa (prawdopodobieństwo zainicjowania pęknięć zmęczeniowych). W okresie eksploatacji obiektu mostowego, skumulowane zmęczenie wzrasta z czasem w różnym tempie, w zależności od poziomu ruchu (ilość cykli) ciężaru wagonów i nacisków na oś (amplituda naprężenia). Wszystkie te czynniki należy określić, aby uzyskać dokładne wyniki analizy niezawodności. Metodą probabilistyczną szacuje się liczbę cykli skumulowanego ruchu pod względem prawdopodobieństwa wykrycia pęknięcia zmęczeniowego. Analiza niezawodności może być wykorzystana do oszacowania pozostałego okresu użytkowania mostu o różnych poziomach bezpieczeństwa.

Metodę można również zastosować do bardziej złożonych konstrukcji, takich jak mosty z belkami poprzecznymi i kratownice. Połączenie między podłużnicą a belką poprzeczną ma pewien stopień sztywności obrotowej, która powoduje koncentrację naprężeń pod wpływem momentu zginającego [38] – połączenia te należy zweryfikować uwzględniając wytrzymałość zmęczeniową, która obejmuje złożony stan naprężeń spowodowany ścinaniem i zginaniem.

Zgodnie z obliczeniami AREMA i Eurokodu bezpieczeństwo zmęczeniowe przęsła o długości 9,75 metra rozważane w tym artykule zostało już przekroczone. Jednak przęsło jest nadal używane bez konieczności wzmacniania, nie odnotowano żadnych uszkodzeń mimo dodatkowych cykli naprężeń spowodowanych zwiększonym naciskiem osi (36 ton). Przykład ten potwierdza, że weryfikacja zmęczenia oceniana aktualnymi metodami jest zbyt zachowawcza. Przedstawione w niniejszej pracy przykłady oraz przykłady innych badaczy (np. [24]) potwierdzają, że weryfikacja nośności konstrukcji nie zależy od wieku konstrukcji, ale od jej aktualnego stanu technicznego oraz widma obciążenia eksploatacyjnego, jakie było, jest i jakie będzie w przyszłości. Należy pamiętać, że parametry materiałowe są istotne w procesie weryfikacji zmęczenia. Dlatego potrzebna jest ocena właściwości materiału w celu określenia prawidłowej charakterystyki stali konstrukcyjnej, zwłaszcza z obiektów historycznych, gdzie właściwości stali są często nieznane. Zależność SN, opracowana i wykorzystana w tym artykule, została określona na podstawie danych z mostów zlokalizowanych w USA i wykonanych ze stali ASTM A373 (obecnie A36/A36M) i może nie być odpowiednia do przewidywania zachowania zmęczeniowego starych mostów metalowych w Europie. Zalecane są dalsze badania w celu oceny przewidywania zmęczenia mostów nitowanych w Europie przy użyciu metody probabilistycznej.

Received: 2021-06-21, Revised: 2021-09-15